Advance Publication

Experimental Animals

Received: 2018.11.19

Accepted: 2019.1.31

J-STAGE Advance Published Date: 2019.3.1

Model animals

Original Paper

Distribution of atherosclerotic lesions in various arteries of WHHLMI rabbits, an animal model of familial hypercholesterolemia

Running head: ATHEROSCLEROSIS OF WHHLMI RABBITS

Takayuki NAKAGAWA[1)*], Akio KIKUMORI[2)], Norie KIMURA[1)], and Masashi SHIOMI[1,2)]

[1)] Division of Comparative Pathophysiology, Kobe University Graduate School of Medicine, 7-5-1, Kusunoki-cho, Chuo-ku, Kobe 650-0017, Japan

[2)] Institute for Experimental Animals, Kobe University Graduate School of Medicine, 7-5-1, Kusunoki-cho, Chuo-ku, Kobe 650-0017, Japan

Corresponding author: Masashi Shiomi

Institute for Experimental Animals, Kobe University Graduate School of Medicine, 7-5-1, Kusunoki-cho, Chuo-ku, Kobe 650-0017, Japan

ieakusm@med.kobe-u.ac.jp

* Present address: Central Research Laboratories, Nichinichi Pharmaceutical Corporation Ltd., Tominaga, Iga, Mie, Japan.

Abstract

In WHHLMI rabbits, arterial lesions develop spontaneously in various arteries even with standard chow. Here, we examined the development of arterial lesions in various arteries to demonstrate standard characteristics of arterial lesions in WHHLMI rabbits. For WHHLMI rabbits at 6, 12, 20, and 30 months of age, lesion areas and areas of arterial lumen surfaces were measured using image analysis software. Histopathological sections of arterial lesions were stained with elastic van Gieson staining. Arterial lesions developed around bifurcations and expanded with aging. In the aorta, atheromatous lesions were severe in the thoracic aorta but were mild in the distal part of the abdominal aorta. Carotid artery lesions progressed in the proximal region and at bifurcations, and the histopathological features were similar to those of coronary lesions. Pulmonary artery lesions contained many foam cells. Fibrous lesions were observed in the proximal and distal areas of the renal arteries, at the bifurcation of the iliac-femoral artery and mesenteric artery, and around the anastomosis of vertebral arteries. Lesions in the celiac artery contained foam cells and/or lipid droplets within fibrous lesions. In a pair of right and left arteries, the arterial lesions tended to progress more in the right artery. Gender did not affect analysis of arterial lesions. In conclusion, the arterial lesions expanded

from bifurcations, and the morphological features of the arterial lesions varied depending on the type of artery. These results serve as reference data for arterial lesions in studies using WHHLMI rabbits.

Key words: atherosclerosis, various arteries, WHHLMI rabbits

Introduction

Atherosclerosis causes many diseases, such as acute coronary syndromes [4, 8], cerebrovascular diseases [2, 9], ischemic nephropathy [1], gastric ischemia [20], and peripheral artery disease [5]. However, there are few studies using laboratory animals with spontaneous arterial lesions in the major arteries of the whole body. The WHHLMI rabbit is an animal model produced by selective breeding of WHHL rabbits [23], and arterial lesions spontaneously develop in various arteries, including coronary arteries, even when feeding standard chow. Although detailed examination of coronary lesions in this rabbit has been reported [30], no detailed examination of arterial lesions on other arteries has been reported. The colony of WHHLMI rabbits at Kobe University was closed, but the WHHLMI rabbit strain is maintained at several research institutes in several countries. Because the characteristics of an animal model should not differ depending on the research institute, it is important to demonstrate standardized characteristics in WHHLMI rabbits. Here, we examined the development of arterial lesions and representative histopathological features in various arteries to serve as reference data for arterial lesions in studies using WHHLMI rabbits.

Materials and Methods

Animals

We used 37 WHHLMI rabbits aged 6–30 months old to examine the distribution of arterial lesions and histopathological features. Rabbits were bred at the Institute for Experimental Animals, Kobe University Graduate School of Medicine. They were housed individually in metal cages (550 mm × 600 mm × 450 mm for width x depth x height) with a flat metal floor and fed standard rabbit chow (LRC4, Oriental Yeast Co., Ltd., Tokyo, Japan) at 120 g/day. The animals were maintained under SPF conditions with a constant temperature (22 ± 2°C), relative humidity (50–60%), ventilation rate (15 cycles/hour), air supply (through a HEPA filter), and lighting cycle (12-h light/dark). This study was approved by the Kobe University Animal Care and Use Committee (approval numbers: P150501, P110511-R1, and P140501), and all animal experiments were conducted in accordance with the Regulations for Animal Experimentation of Kobe University, the Act on Welfare and Management of Animals (Law No. 105, 1973, revised in 2006), Standards Relating to the Care and Management of Laboratory Animals and Relief of Pain (Notification No. 88, 2006), and Fundamental Guidelines for the Proper Conduct of Animal Experiments and Related Activities in Academic Research Institutions under the Jurisdiction of the

Ministry of Education, Culture, Sports, Science and Technology (Notice No. 71, 2006).

Evaluation of arterial lesions

The extent of arterial lesions was evaluated macroscopically as a percentage of the surface lesion area by dividing the lesion area on the surface of the arterial lumen by the surface area of the arterial lumen. Detailed methods are shown in Supplementary Figure 1 to Supplementary Figure 5. Although there were differences in the percentage of the surface lesion area between females and males in some segments of the arteries, the percentages of the surface lesion area were reversed between females and males or similar in females and males at adjacent segments or at ages that were younger or older than the analysis age (Supplementary Table 1 to Supplementary Table 7). These results indicate that the difference in the percentage of the surface lesion area between females and males does not seriously affect the analysis of lesion progression with aging. Therefore, changes in arterial lesions due to aging were examined using both females and males.

Preparation of histopathological sections for arterial lesions

Arteries and hearts were extracted after euthanasia by intravenous injection of

pentobarbital sodium solution (100 mg/kg). The arteries were immersion-fixed in 10% buffered neutral formalin solution. Arterial sections were prepared from the thoracic aorta, the proximal area of the carotid artery, the pulmonary trunk, the proximal area of the renal artery, the proximal area of the celiac artery, the proximal area of the mesenteric artery, near the anastomotic site of the vertebral arteries, and the left circumflex coronary arteries. Coronary sections and cerebral sections were prepared by a method reported previously [13, 22]. Sections were stained with elastic van Gieson staining.

Other assays

After more than 12 h of fasting, total cholesterol and triglyceride levels in serum were assayed by dry chemistry using a Fuji DRI-CHEM 3500SV (Fuji Film Co., Ltd., Tokyo, Japan) [29].

Statistical analyses

Data are presented as the mean ± standard error of the mean (SEM). Statistical analyses were performed on mean values with Student's t-test, Welch's t-test, or the Tukey test. A value of $P<0.05$ was considered significant.

Results

Serum lipid levels of WHHLMI rabbits

Supplementary Table 8 shows the serum lipid levels of the WHHLMI rabbits. The serum cholesterol level was 1131 ± 29 mg/dl in females and 1122 ± 30 mg/dl in males at 6 months old, and it then gradually decreased with aging. The serum cholesterol level decreased faster in males than in females. The serum triglyceride level showed no gender differences and no age-dependent decreases.

Distribution of arterial lesions on the aorta

Figure 1 shows the distribution of aortic lesions at each age. The percentage of the surface lesion area became smaller as close to the distal portion at each age. Excluding the distal part of the abdominal aorta (segments A-4 to A-7), aortic lesions progressed with aging (Supplementary Table 9).

Distribution of arterial lesions on the carotid arteries

Figure 2 shows the distribution of lesions at carotid arteries. Arterial lesions were observed in the proximal region, around the orifice of the anterior thyroid artery,

and in the carotid sinus and progressed with aging (Supplementary Table 10). At 12 months old, the percentage of the surface lesion area was higher in the left carotid artery than in the right carotid artery, whereas at 20 months old and 30 months old, the percentage was higher in the right carotid artery than in the left carotid artery (Supplementary Table 11).

Distribution of arterial lesions on the pulmonary arteries

Figure 3 shows the distribution of arterial lesions on pulmonary arteries. Pulmonary lesions were frequently observed in the pulmonary trunk, pulmonary sinus, and right pulmonary arteries and progressed with aging (Supplementary Table 12). The percentage of the surface lesion area was higher in the right pulmonary artery than in the left pulmonary artery (Supplementary Table 13).

Distribution of arterial lesions on the renal arteries

Figure 4 shows arterial lesions of renal arteries. Lesions in the proximal and distal parts were larger than in the middle part, and lesion area increased with aging (Supplementary Table 14). The percentage of the surface lesion area was higher in the right renal artery than in the left renal artery (Supplementary Table 13).

Distribution of arterial lesions on the iliac-femoral arteries

Figure 5 shows the arterial lesions of the iliac-femoral arteries. Lesions were observed in rabbits aged more than 19 months old (Supplementary Table 15). The lesions were observed at common iliac arteries, around the internal iliac artery branch, and around the deep femoral artery branch. At 20 months old, the percentage of the surface lesion area was higher in the right iliac-femoral artery than in the left iliac-femoral artery, but there was no difference at 30 months old (Supplementary Table 16).

Difference in features of arterial lesions depending on artery type

Figure 6 shows photomicrographs of arterial lesions in various arteries. Macrophage-rich lesions were observed in pulmonary arteries. Lesions with a lipid core covered by a fibrous cap were observed in thoracic aortas, carotid arteries, and coronary arteries. Calcium accumulation was also observed in aortic lesions. Lesions on the distal area of the abdominal aorta were relatively fibrous (data not shown). Carotid and coronary lesions with various features, such as fibrous lesions, layered lesions with layers of fibrous components and layers with lipid components, and

other types of lesions, were also observed (Figure 6). Celiac lesions contained foam cells and/or lipid droplets within the fibrous lesions. Lesions observed in the renal arteries, mesenteric arteries, and vertebral arteries were fibrous lesions. Lesions observed in the iliac-femoral arteries were also fibrous lesions (data not shown).

Discussion

In the present study, we examined arterial lesions in various arteries of WHHLMI rabbits to provide reference data for arterial lesions in studies using WHHLMI rabbits. This is the first systematic examination of lesion sites and histopathological features of various arteries. Arterial lesions were frequently observed around bifurcations, and histopathological features varied greatly depending on the artery.

For aortic lesions, thoracic lesions were more advanced than abdominal lesions, and the lesions distal to the left renal artery orifice (from segment A-4 to segment A-7) were mild. In humans who died as a result of accidents, aortic lesions were located around the intercostal ostia and the origin of the superior mesenteric and celiac arteries, and the lesions covered 5–40% of the aortic surface [24]. In addition, atherosclerotic lesions are frequently observed in the abdominal aorta not only at

the visceral artery branching site [27] but also in the area of the terminal abdominal aorta [6]. Therefore, the predominant site of lesions in WHHLMI rabbits was different from that in humans. In patients with familial hypercholesterolemia, the aorta is covered throughout with atherosclerotic lesions, and lesions are more severe in the ascending aorta than in the thoracic and abdominal aorta [31]. Those aortic lesions are composed of various amounts of fibrous tissue, inflammatory cells, cholesterol clefts, and foam cells [31]. The extent of lesion spread and lesion composition are similar between WHHLMI rabbits and humans, especially for familial hypercholesterolemia.

Carotid lesions were frequently observed in the area of the carotid sinus and the proximal area of the carotid artery. These findings are similar to those of human carotid lesions [6]. Carotid artery lesions with various histopathological features, such as fibrous lesions, atheromatous lesions, and lesions with a lipid core covered with a thin fibrous cap, were observed, as in the case of coronary lesions [21, 30]. The histopathological features of carotid artery lesions in humans resembled those of WHHLMI rabbits [12, 16]. In addition, the composition of carotid plaques in humans is associated with coronary plaque composition [16], future onset of acute coronary syndromes [10], and stroke [26]. The features of carotid lesions in WHHLMI rabbits

were similar to those of humans.

In vertebral arteries, fibrous lesions with less than 50% narrowing were observed in WHHLMI rabbits, which was consistent with results from WHHL rabbits, a previous strain of WHHLMI rabbits [12]. In patients with familial hypercholesterolemia, cerebral arterial lesions are composed of fibrous components with no macrophage infiltration and are mild compared with aortic and coronary lesions [31]. The features of vertebral artery lesions in WHHLMI rabbits were similar to those of humans, but there are no animal models of spontaneous cerebral atherosclerosis.

The pulmonary artery lesions exhibited marked accumulation of macrophages and foam cells. However, Hansen et al. [11] reported that pulmonary lesions are fibrous or advanced in WHHL rabbits. Higher serum lipid levels in WHHLMI rabbits than in WHHL rabbits [23] may be responsible for the macrophage-rich lesions in pulmonary arteries. In humans, pulmonary lesions are detected by echocardiography at the main trunk and right pulmonary artery, but these lesions are not correlated with clinical findings [19].

The renal artery lesions were mainly fibrous lesions in WHHLMI rabbits and were observed in the proximal area just after branching from the abdominal aorta.

Kamimura et al. [15] reported intimal thickening in renal arteries at the hilum of the kidney in WHHL rabbits. In humans, most renal artery lesions are fibrous [16], but some renal arteries also have atherosclerotic lesions [7]. These lesions occur mainly in the proximal one-third of the renal artery [14]. Chronic renal failure develops within 6 years in up to 27% of patients with atherosclerotic renal artery stenosis [28], and these patients have a higher incidence of acute coronary syndromes [9]. Renal artery stenosis is an important disease, but there are no animal models besides WHHL and WHHLMI rabbits that spontaneously develop the disease.

Layered lesions with foam cells and/or lipid droplets within fibrous lesions were observed in the proximal area of the celiac artery and superior mesenteric artery in WHHLMI rabbits. In humans, these lesions consist of fatty streaks, fibrolipid lesions, and complicated lesions [17]. Downstream of the celiac artery, splenic artery, common hepatic artery, pancreatic artery, gastric artery, and superior mesenteric artery are other arteries in the pancreaticoduodenal area and mesentery. Fibrocellular intimal thickening of the superior pancreaticoduodenal artery may cause focal pancreatic changes under ischemic conditions [25], and celiac or mesenteric stenosis causes gastric ischemia in humans [20]. Therefore, WHHLMI rabbits may be an animal model of gastric ischemia.

Fibrous lesions were observed in the common iliac artery and large branching sites in the iliac-femoral artery in WHHLMI rabbits. In humans, arterial lesions are frequently observed in the iliac-femoral artery [6]. Most peripheral artery lesions are fibrous lesions, such as pathological intimal thickening and fibrocalcific lesions, and atheromatous lesions are rare [16]. The risk factors for these lesions are smoking and diabetes rather than hypercholesterolemia [3]. Therefore, fibrous lesions observed in the iliac-femoral arteries of WHHLMI rabbits may be different from those in humans.

Differences between lesions that developed in the right and left pairs of arteries, such as in the carotid artery and renal artery, may have resulted from changes in blood flow because of differences in branch location and the distribution of other branches in the surrounding area. In WHHLMI rabbits, the features of the arterial lesions depended on the artery, which is similar to humans [16]. Various factors, such as the structure or thickness of the arterial wall, blood pressure in the arteries, arterial curvature [18], or other unknown factors, may explain differences in lesion features in different arteries.

In the present study, we examined the development of arterial lesions in the major arteries of WHHLMI rabbits. The arterial lesions expanded from bifurcations,

and the morphological features of the arterial lesions varied from artery to artery. These results will provide reference data for arterial lesions in studies using WHHLMI rabbits.

Conflict of interests

The authors declare no competing interests.

Sources of funding

This study was partly supported by a Grant-in-Aid for Scientific Research from the Ministry of Education, Culture, Sports, Science and Technology, Japan (23300157 to Masashi Shiomi).

Acknowledgments

We would like to express our appreciation to Mr. Takashi Ito for preparing histopathological sections of various arteries.

References

1. Adamczak, M. and Wiecek A. 2012. Ischemic nephropathy - pathogenesis and

treatment. *Nefrologia.* 32: 432-438.

2. Al Kasab, S., Derdeyn, C.P., Guerrero, W.R., Limaye, K., Shaban, A., and Adams, H.P. Jr. 2018. Intracranial Large and Medium Artery Atherosclerotic Disease and Stroke. J Stroke *Cerebrovasc. Dis*. 27:1723-1732.

3. Allaqaband, S., Kirvaitis, R., Jan, F., and Bajwa, T.2009. Endovascular treatment of peripheral vascular disease. *Curr. Probl. Cardiol.* 34:359-476.

4. Crea, F., and Libby, P. 2017. Acute Coronary Syndromes: The Way Forward From Mechanisms to Precision Treatment. *Circulation*. 136:1155-1166.

5. Criqui, M.H., and Aboyans, V. 2015. Epidemiology of peripheral artery disease. *Circ. Res*. 116:1509-1526.

6. DeBakey, M.E., Lawrie, G.M., and Glaeser, D.H. 1985. Patterns of atherosclerosis and their surgical significance. *Ann Surg*.201:115-31.

7. Dubel, G.J., and Murphy, T.P. 2008. The role of percutaneous revascularization for renal artery stenosis. *Vasc. Med*. 13:141-156.

8. Edwards, M.S., Craven, T.E., Burke, G.L., Dean, R.H., and Hansen, K.J. 2005. Renovascular disease and the risk of adverse coronary events in the elderly: a prospective, population-based study. *Arch. Intern. Med*. 165:207-213.

9. Finn, C., Giambrone, A.E., Gialdini, G., Delgado, D., Baradaran, H., Kamel, H.,

and Gupta, A. 2017. The Association between Carotid Artery Atherosclerosis and Silent Brain Infarction: A Systematic Review and Meta-analysis. *J. Stroke .Cerebrovasc. Dis.* 26:1594-1601.

10. Hamada, S., Kashiwazaki, D., Yamamoto, S., Akioka, N., Kuwayama, N., and Kuroda, S. 2018. Impact of Plaque Composition on Risk of Coronary Artery Diseases in Patients with Carotid Artery Stenosis. *J. Stroke. Cerebrovasc. Dis.* S1052-3057(18)30485-3.

11. Hansen, B.F., Mortensen, A., Hansen, J.F., Ibsen, P., Frandsen, H., and Nordestgaard, B.G. 1994. Atherosclerosis in Watanabe heritable hyperlipidemic rabbits. *APMIS* 1102:177-190

12. Holm, J., and Hansson, GK. 1990. Cellular and immunologic features of carotid artery disease in man and experimental animal models. *Eur Jvasc Surg.* 4:49-55

13. Ito, T., and Shiomi, M. 2001. Cerebral atherosclerosis occurs spontaneously in homozygous WHHL rabbits. *Atherosclerosis* 156: 57-66.

14. Kaatee, R., Beek, F.J., Verschuyl, E.J., vd Ven, P.J., Beutler, J.J., van Schaik, J.P., and Mali, W.P. 1996. Atherosclerotic renal artery stenosis: ostial or truncal? *Radiology.* 199:637-640.

15. Kamimura, R., Suzuki, S., Miyahara, K., and Shiomi, M. 2001. Arteriosclerosis

in the influx and intravisceral arteries of the liver, kidney and lung of WHHL rabbits. *Exp. Anim.* 50: 423-426.

16. Matsuo, Y., Takumi, T., Mathew, V., Chung, W.Y., Barsness, G.W., Rihal, C.S., Gulati, R., McCue, E.T., Holmes, D.R., Eeckhout, E., Lennon, R.J., Lerman, L.O., and Lerman, A. 2012. Plaque characteristics and arterial remodeling in coronary and peripheral arterial systems. *Atherosclerosis* 223:365-371.
17. Naeem, A., Nasim, N., Ihsan, U., and Masood, A. 2012. A morphological study of celiac, superior mesenteric and inferior mesenteric arteries in atherosclerosis. *J. Ayub. Med. Coll. Abbottabad.* 24:18-21.
18. Nagasaka, R., Koike, T., Tsukada, N., Tamura, S., and Shiomi, M. 2018.The coronary artery running pattern is one of the causes of individual differences in the progression of coronary atherosclerosis in WHHLMI rabbits, an animal model for coronary atherosclerosis. *J. Atheroscler. Thromb.* 25:393-404.
19. Russo, A., De Luca, M., Vigna, C., De Rito, V., Pacilli, M., Lombardo, A., Armillotta, M., Fanelli, R., and Loperfido, F. 1999. Central Pulmonary Artery Lesions in Chronic Obstructive Pulmonary Disease. *Circulation* 100:1808-1815.
20. Saldaña Dueñas, C., Elosua González, A., and Guerra Lacunza, A. 2018. Gastric ischemia due to critical stenosis of the celiac trunk. *An. Sit. Sanit. Navar.* 41:123-

127.

21. Shiomi, M., Ishida, T., Kobayashi, T., Nitta, N., Sonoda, A., Yamada, S., Koike, T., Kuniyoshi, N., Murata, K., Hirata, K.I., Ito, T., and Libby, P. 2013. Vasospasm .of Atherosclerotic Coronary Arteries Precipitates Acute Ischemic Myocardial Damage in Myocardial Infarction-Prone Strain of the Watanabe Heritable Hyperlipidemic Rabbits. *Arterioscler. Thromb. Vasc. Biol.* 33: 2518-2523.

22. Shiomi, M., Ito, T., Shiraishi, M., and Watanabe, Y. 1992. Inheritability of atherosclerosis and the role of lipoproteins as risk factors in the development of atherosclerosis in WHHL rabbits: risk factors related to coronary atherosclerosis are different from those related to aortic atherosclerosis. *Atherosclerosis* 96: 43–52.

23. Shiomi, M., Ito, T., Yamada, S., Kawashima, S., and Fan, J. 2003. Development of an animal model for spontaneous myocardial infarction (WHHLMI rabbit). *Arterioscler. Thromb. Vasc. Biol.* 23: 1239-1244.

24. Svindland, A., and Walløe, L. 1985. Distribution pattern of sudanophilic plaques in the descending thoracic and proximal abdominal human aorta. *Atherosclerosis.* 57:219-224.

25. Uchida, T., Tsuchiya, R., Harada, N., Tsunoda, T., Yamaguchi, T., Eto, T., and

Furukawa, M. 1988. Ischemic changes in the pancreas of Watanabe heritable hyperlipidemic (WHHL) rabbits. *Int. J. Pancreatol.* 3: 261-272.

26. Virmani, R., Burke, A., Ladich, E., and Kologie, F.D. 2006. Pathology of carotid artery atherosclerotic disease. Carotid Disease. The Role of Imaging in Diagnosis and Management. 2006; 1-10. Ed by Gillard, J., Graves, M., Hatsukami, T., and Yuan, C. Cambridge University Press, Cambridge, United Kingdom.

27. Wissler RW. 1991. USA multicenter study of the pathobiology of atherosclerosis in youth. *Ann N Y Acad Sci.* 623:26–39.

28. Wollenweber, J., Sheps, S.G., and Davis, G.D. 1968. Clinical course of atherosclerotic renovascular disease. *Am. J. Cardiol.* 21:60-71.

29. Yamada, S., Ito, T., Tamura, T., and Shiomi, M. 2004. Age related changes in serum/plasma biochemical parameters of WHHLMI rabbits. *Exp. Anim.* 53: 159–163.

30. Yamada, S., Koike, T., Nakagawa, T., Kuniyoshi, N., Ying, Y., Itabe, H., Yamashita, A., Asada, Y., and Shiomi, M. 2017. Morphological features of coronary plaques in WHHLMI rabbits (Oryctolagus cuniculus), an animal model for familial hypercholesterolemia. *Exp. Anim.* 66: 145-157.

31. Yutani, C., Go, S., Imakita, M., Ishibashi-Ueda, H., Hatanaka, K., and Yamamoto, A. 1987. Autopsy findings in two patients with homozygous familial hypercholesterolemia. Special references to apolipoprotein B localization and internalization defect of low density lipoprotein. *Acta. Pathol. Jpn.* 37:1489-1504.

Figure Legends

Figure 1. Distribution of arterial lesions on the aorta in WHHLMI rabbits aged 6 (open circles, 2 females and 5 males), 12 (closed circles, 5 females and males), 20 (open diamonds, 5 females and males), and 30 (closed diamonds, 5 females and males) months old. AsA, ascending aorta; AA, aortic arch; T-1 to T-9, thoracic segments from the proximal to the distal region; A-1 to A-7, abdominal segments from the proximal to the distal region. Error bars indicate the SEM.

Figure 2. Distribution of arterial lesions on carotid arteries in WHHLMI rabbits aged 6 (open circles, 2 females and 5 males), 12 (closed circles, 5 females and males), 20 (open diamonds, 5 females and males), and 30 (closed diamonds, 5 females and males) months old. C-1, proximal area of the carotid artery; C-2, area between C-1 and C-3; C-3, area around the orifice of the anterior thyroid artery; C-4, area between C-3 and C-5; C-5, carotid sinus. Error bars indicate the SEM.

Figure 3. Distribution of arterial lesions on pulmonary arteries in WHHLMI rabbits aged 6 (open columns, 2 females and 5 males), 12 (hatched columns, 5 females and males), 20 (dotted columns, 5 females and males), and 30 (closed columns, 5 females

and males) months old. Error bars indicate the SEM.

Figure 4. Distribution of arterial lesions on renal arteries in WHHLMI rabbits aged 6 (open circles, 2 females and 5 males), 12 (closed circles, 5 females and males), 20 (open diamonds, 5 females and males), and 30 (closed diamonds, 5 females and males) months old. R-1, the proximal area immediately after branching from the abdominal aorta; R-2, area between R-1 and R-3; R-3, the distal area on the kidney side. Error bars indicate the SEM.

Figure 5. Distribution of arterial lesions on iliac-femoral arteries in WHHLMI rabbits aged 6 (open circles, 2 females and 5 males), 12 (closed circles, 5 females and males), 20 (open diamonds, 5 females and males), and 30 (closed diamonds, 5 females and males) months old. I-1, common iliac artery; I-2, the proximal site between the deep iliac artery branch and the internal iliac artery branch; I-3, the distal site between the deep iliac artery branch and the internal iliac artery branch; I-4, internal iliac artery branch; I-5, the proximal site between the internal iliac artery branch and the femoral bifurcation; I-6, the distal site between the internal iliac artery branch and the femoral bifurcation; I-7, femoral bifurcation. Error bars

indicate the SEM.

Figure 6. Microphotographs of arterial lesions on the thoracic aorta, carotid artery, pulmonary artery, renal artery, celiac artery, mesenteric artery, and coronary artery. Arterial sections were stained with elastic van Gieson staining. Red components are collagen fibers, and black components are elastic fibers. 12M, 12 months old; 20M, 20 months old; Ca, calcium accumulation.

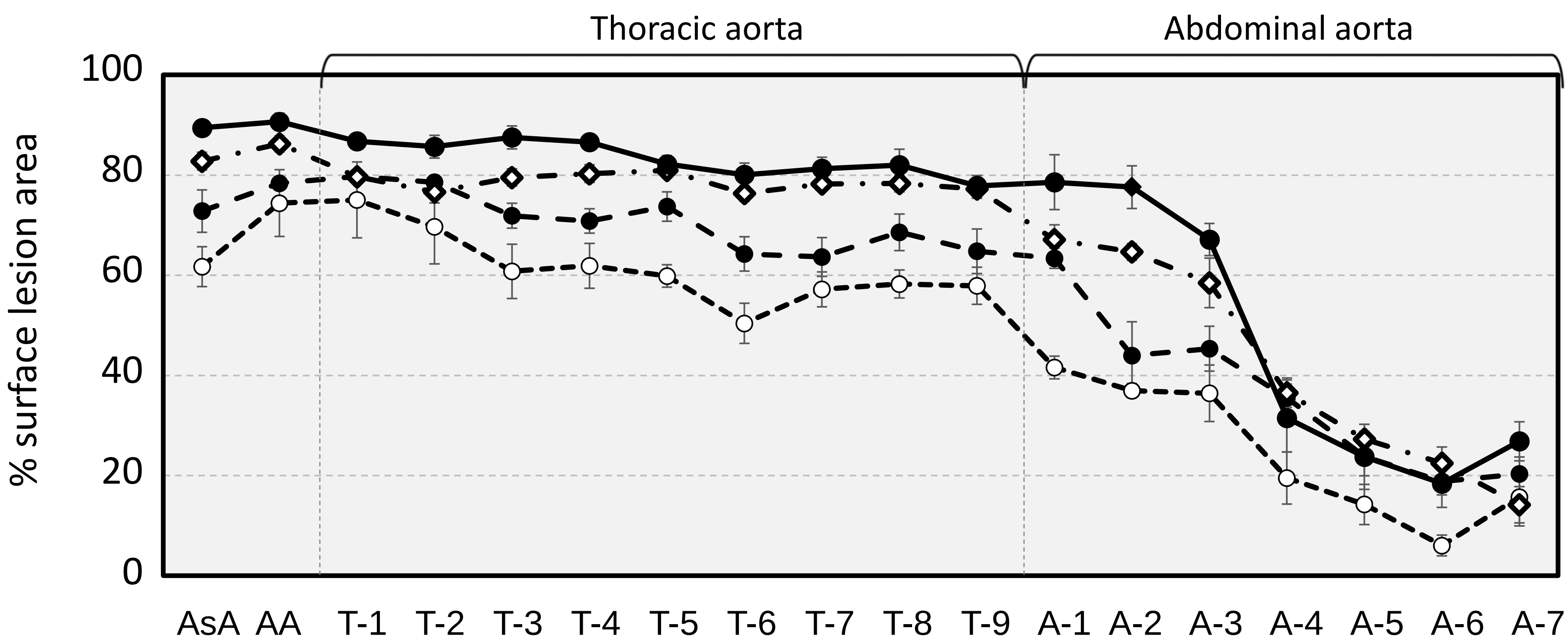
Thoracic aorta
Abdominal aorta
% surface lesion area
100
80
60
40
20
0
AsA
AA
T-1
T-2
T-3
T-4
T-5
T-6
T-7
T-8
T-9
A-1
A-2
A-3
A-4
A-5
A-6
A-7

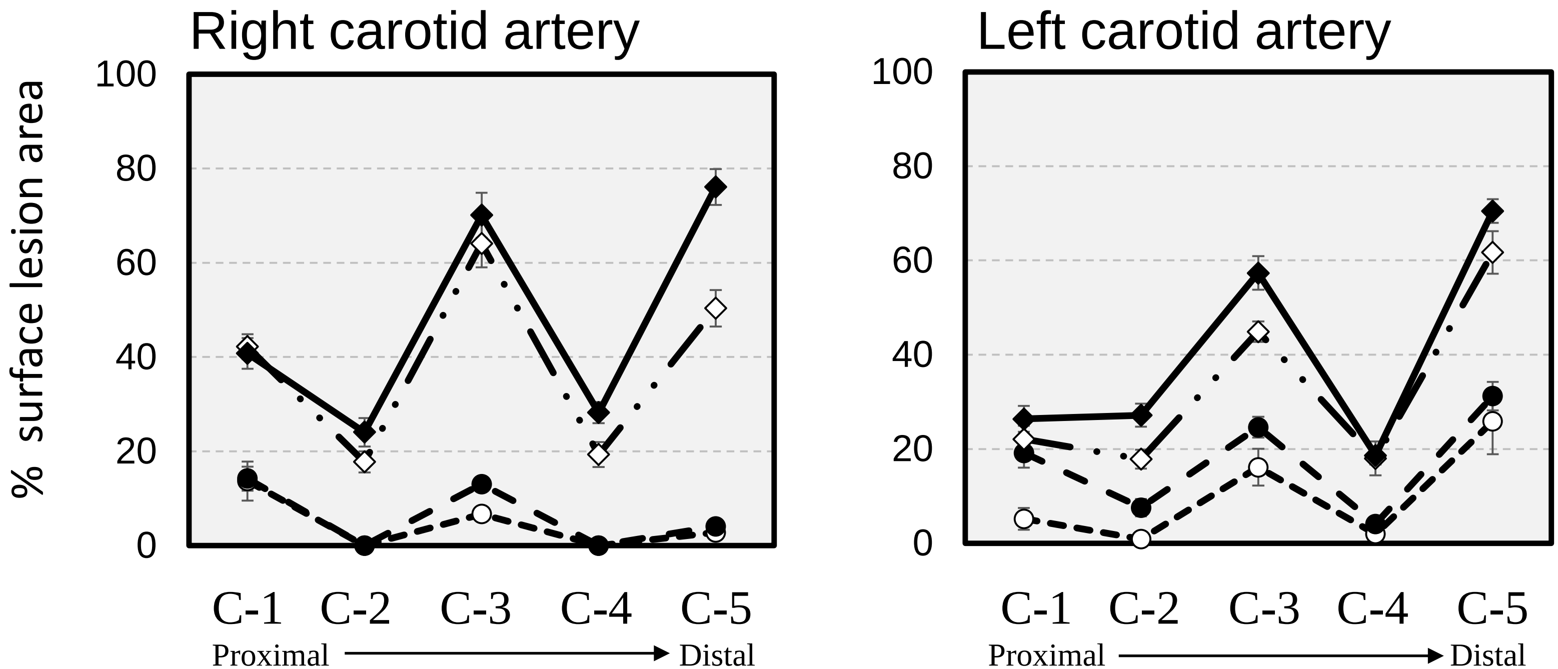

Right carotid artery
Left carotid artery
% surface lesion area
100
80
60
40
20
0
C-1
C-2
C-3
C-4
C-5
Proximal
Distal

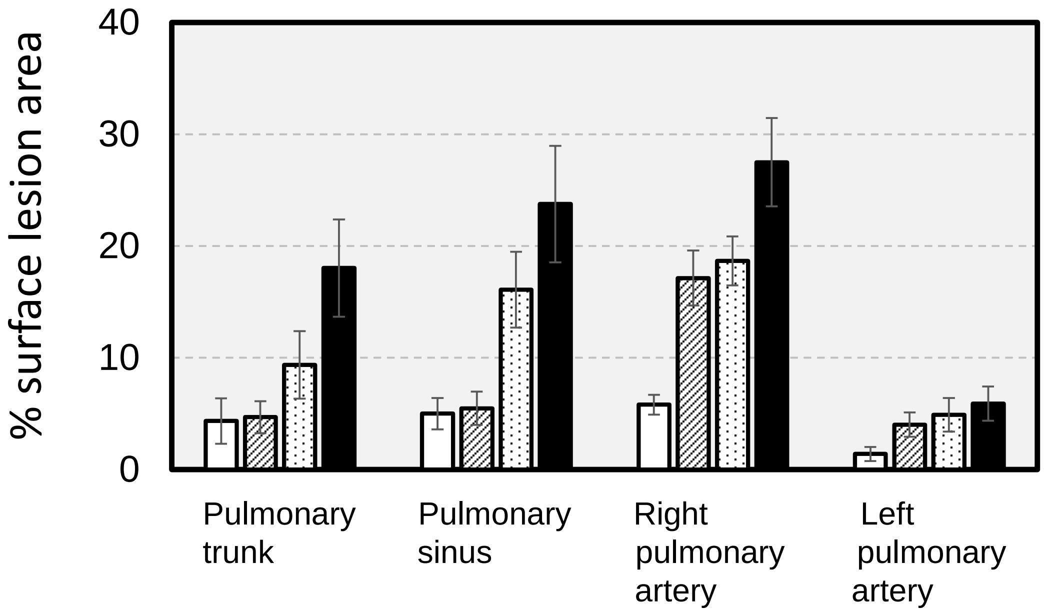

% surface lesion area
40
30
20
10
0
Pulmonary trunk
Pulmonary sinus
Right pulmonary artery
Left pulmonary artery

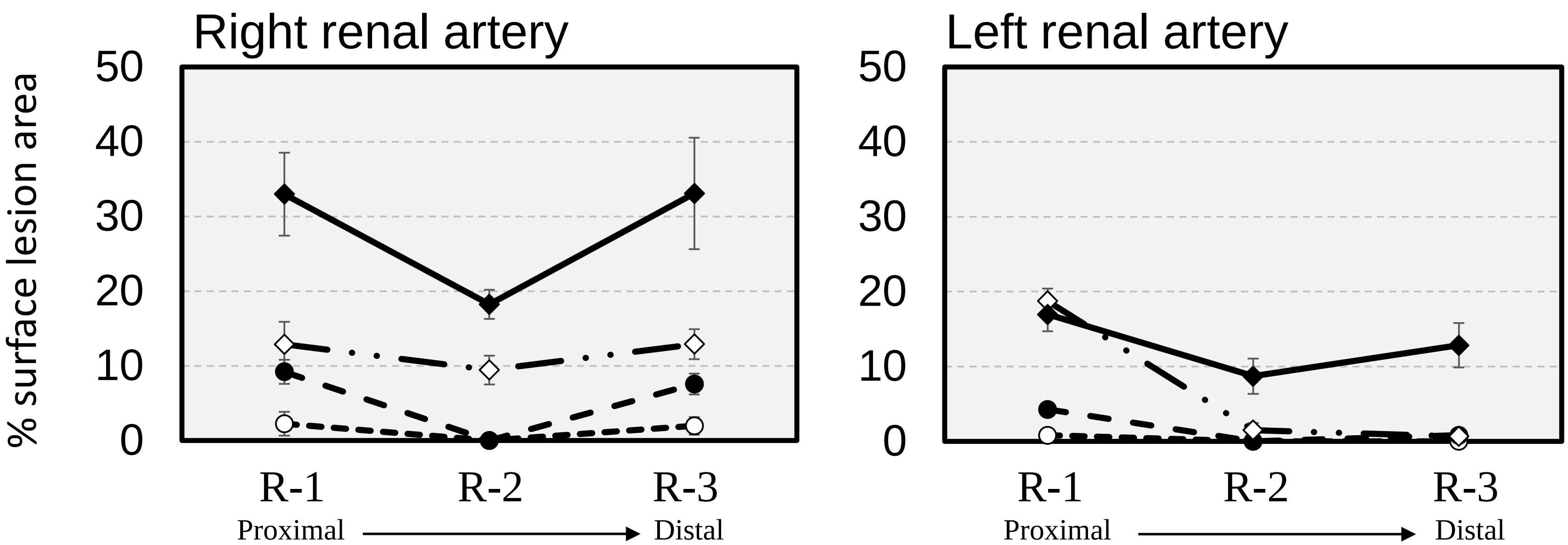

Right renal artery
Left renal artery
% surface lesion area
50
40
30
20
10
0
R-1
R-2
R-3
Proximal
Distal

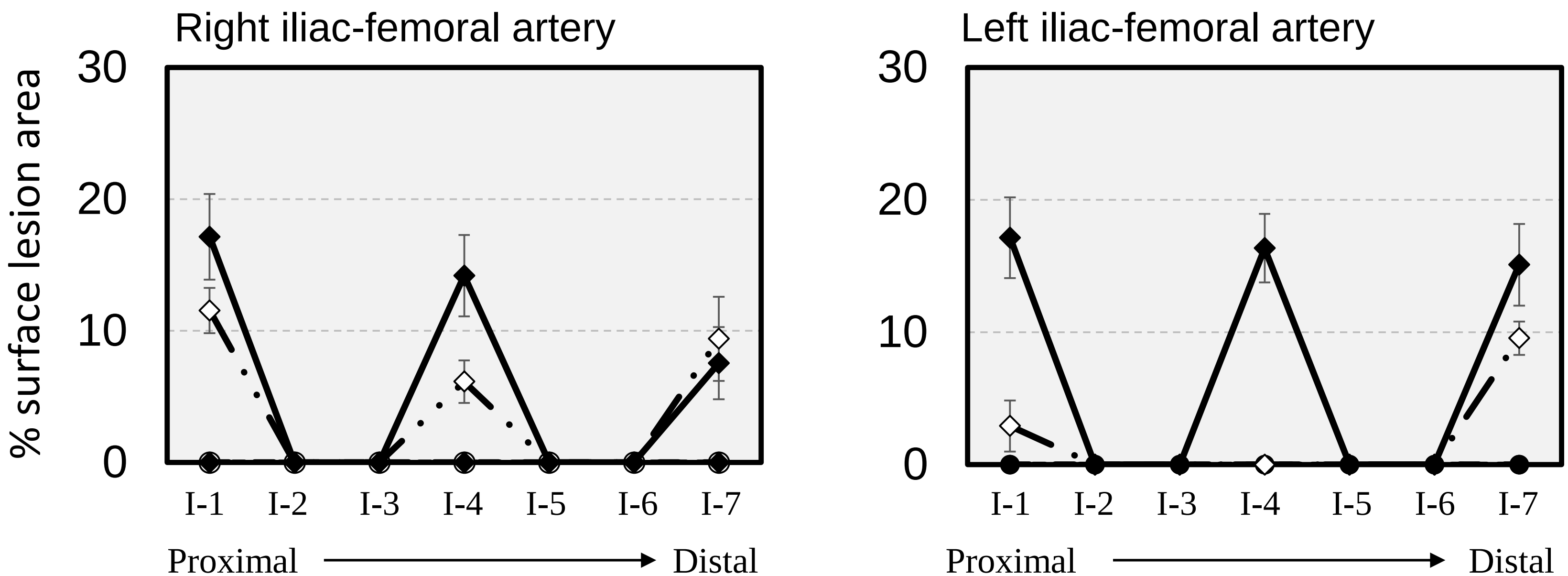

Right iliac-femoral artery
Left iliac-femoral artery
% surface lesion area
30
20
10
0
I-1
I-2
I-3
I-4
I-5
I-6
I-7
Proximal
Distal

Fig 6

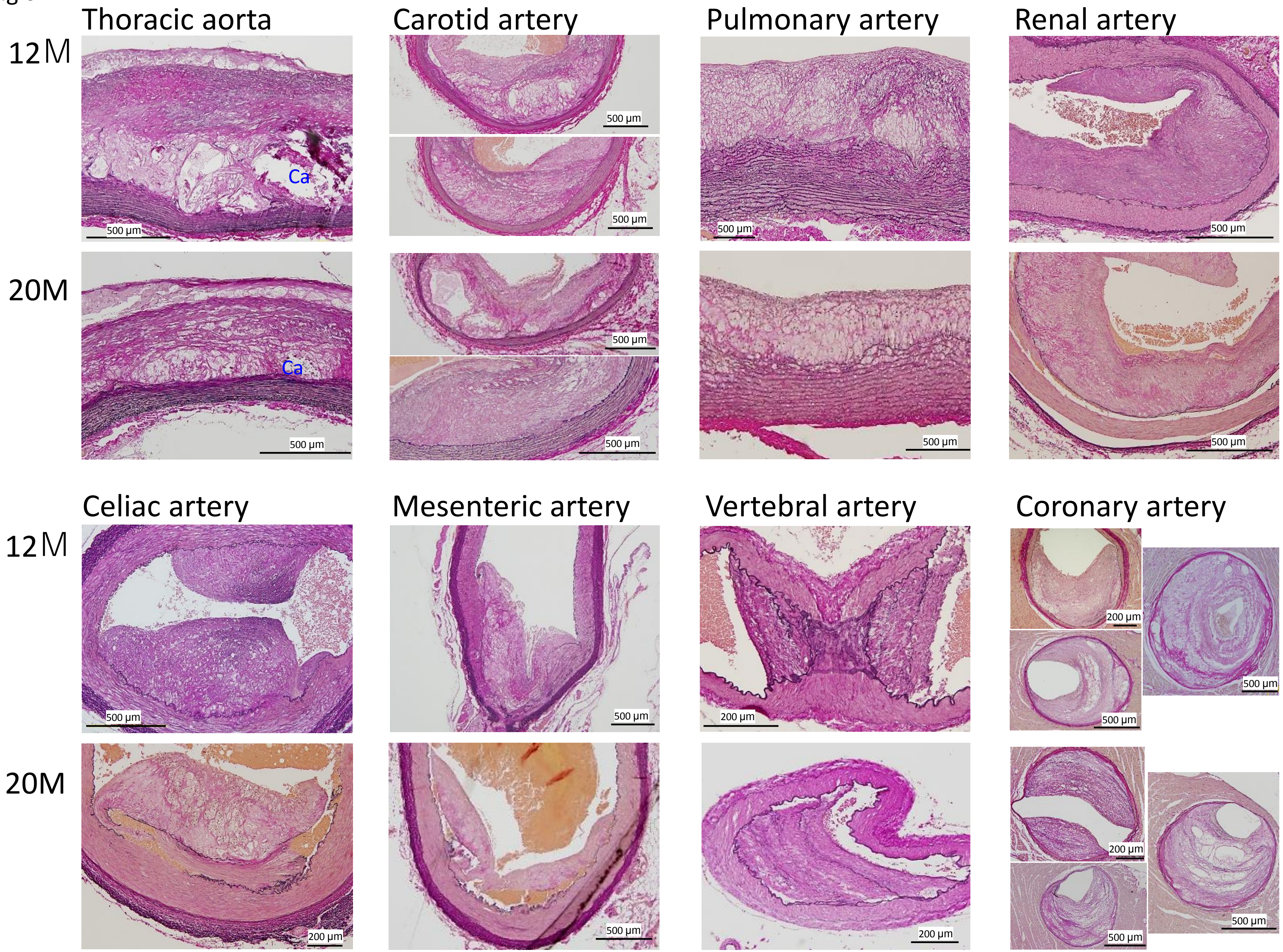

Thoracic aorta
Carotid artery
Pulmonary artery
Renal artery
12M
20M
Ca
Ca
500 µm
Celiac artery
Mesenteric artery
Vertebral artery
Coronary artery
12M
20M
200 µm
500 µm

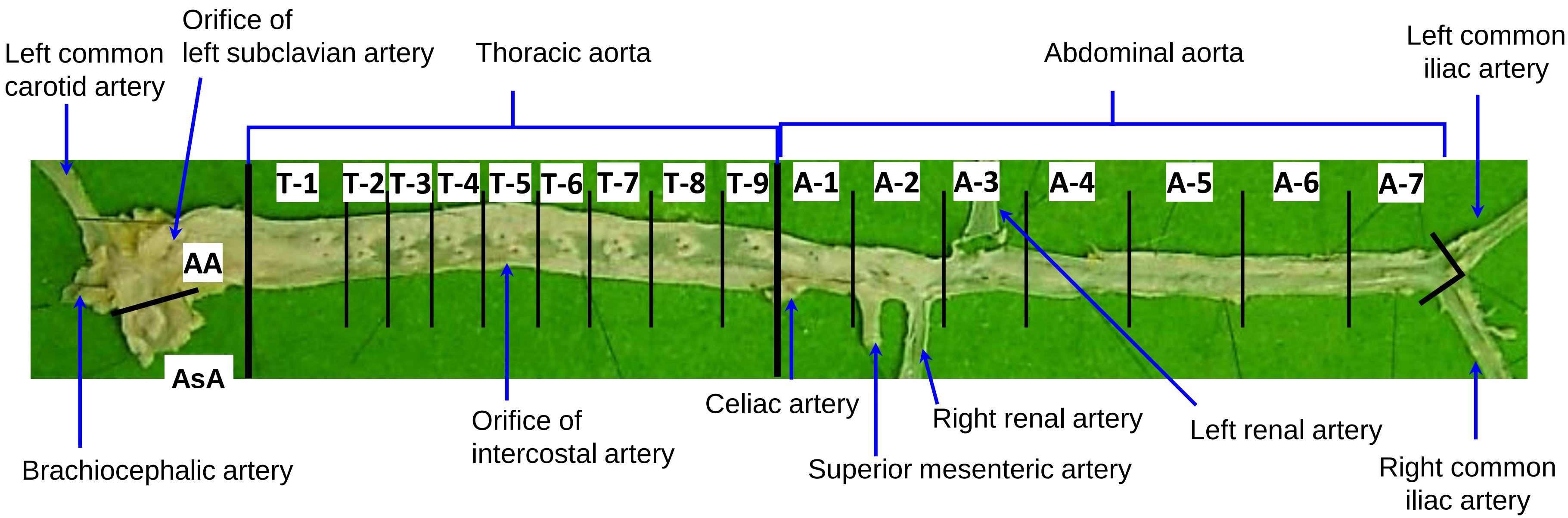

Supplementary Figure 1. Preparation method of aortic segments to evaluate the percentage of the surface lesion area.
The ascending aorta (AsA) was designated as the heart side bisected from the aortic valve area to the orifice of the brachiocephalic artery. The aortic arch (AA) was designated as the area from this boundary to the midpoint between the left subclavian artery and the first intercostal artery. The thoracic aorta (from this boundary to the diaphragm) was divided at the center of each orifice of the intercostal artery and was designated as T-1 to T-9 in order from the origin. For the abdominal aorta, the area from the diaphragm to the orifice of the superior mesenteric artery was designated as A-1. From the orifice of the superior mesenteric artery to the midpoint of the orifice of the right renal artery and the left renal artery was designated as A-2. From this boundary to the midpoint between the orifice of the first lumbar arteries and the orifice of left renal artery was designated as A-3. The sections from this boundary to the femoral artery branch were equally divided into A-4 to A-7.

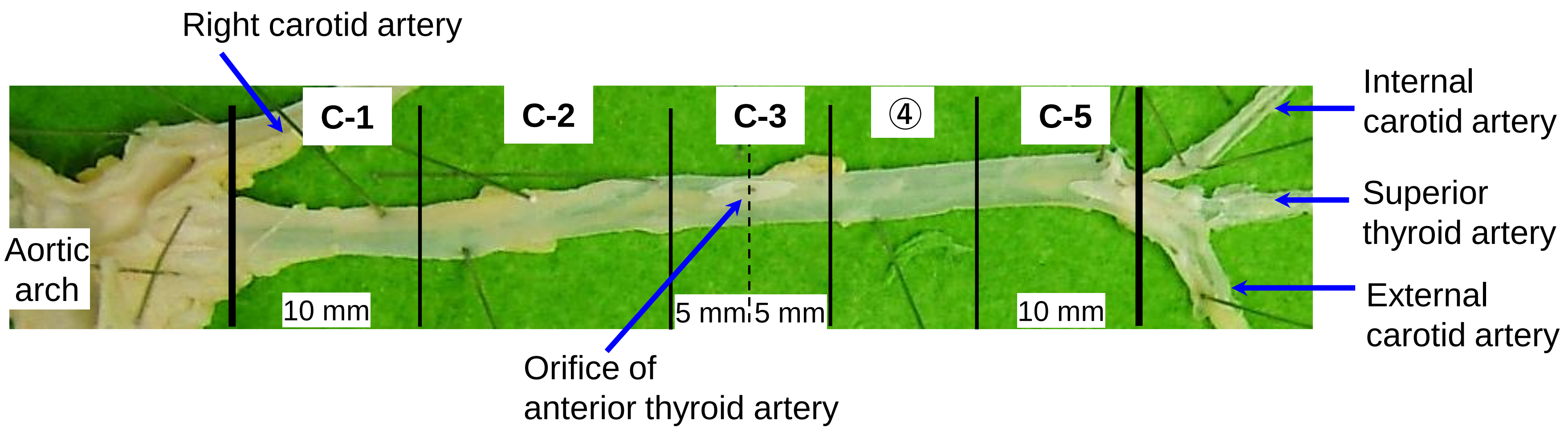

Supplementary Figure 2. Preparation method of the carotid segments to evaluate the percentage of the surface lesion area.

C-1, proximal area of the carotid artery; C-2, area between C-1 and C-3; C-3, area around the orifice of the anterior thyroid artery; C-4, area between C-3 and C-5; C-5, carotid sinus.

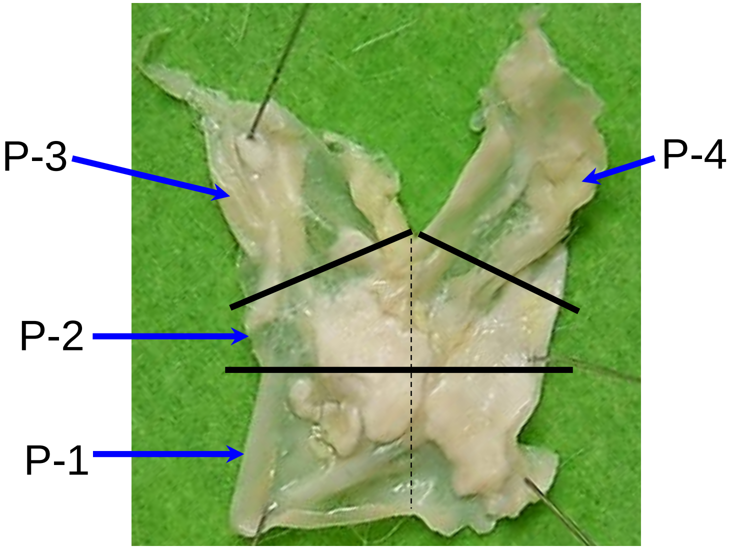

Supplementary Figure 3. Preparation method of pulmonary segments to evaluate the percentage of the surface lesion area.

The area from the pulmonary artery valve to the left and right branch of the pulmonary artery was bisected; the heart side was designated as the pulmonary trunk (P-1), and the branch side was designated as the pulmonary sinus (P-2). P-3, right pulmonary artery; P-4, left pulmonary artery.

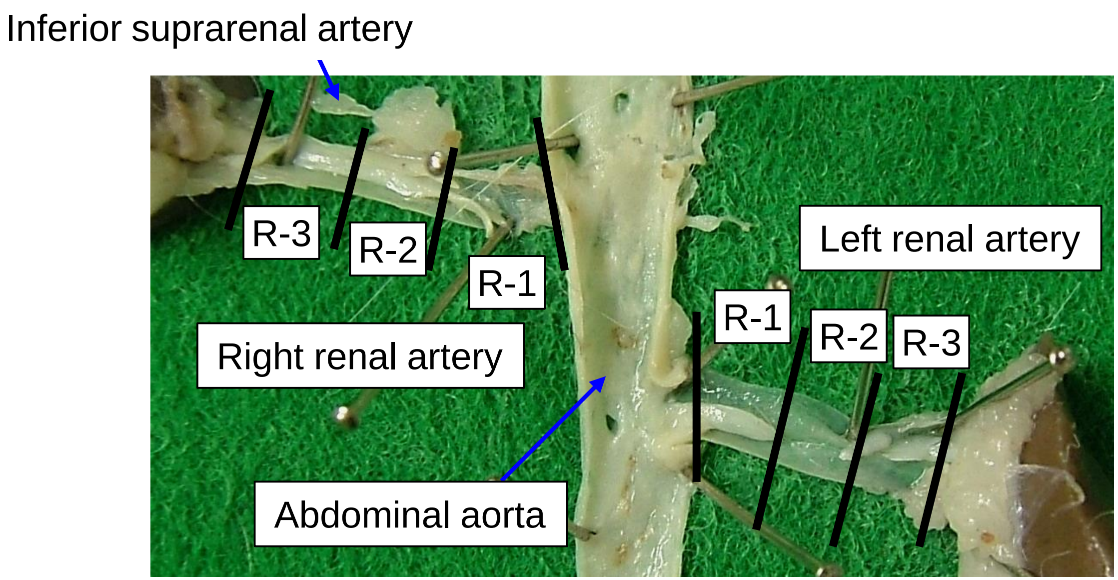

Supplementary Figure 4. Preparation method of renal segments to evaluate the percentage of the surface lesion area. Renal arteries were equally divided into 3 segments: the proximal area (R-1) immediately after branching from the abdominal aorta, the distal area (R-3) on the kidney side, and the area between them (R-2).

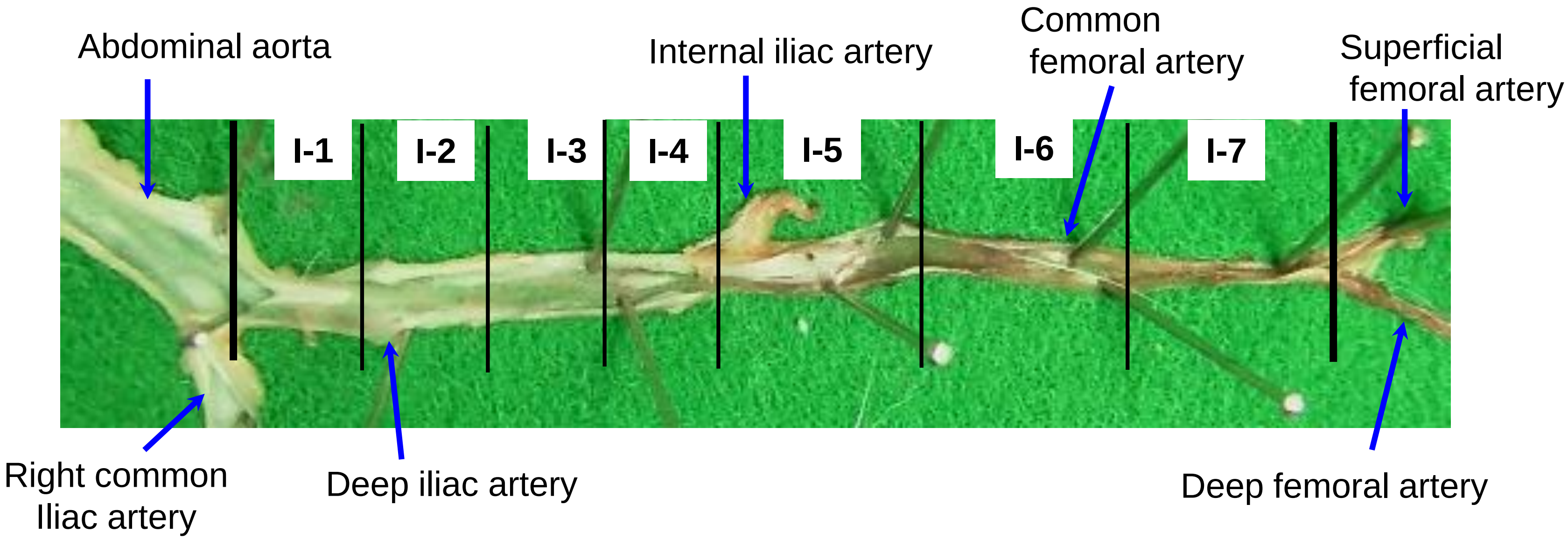

Supplementary Figure 5. Preparation method of segments of the iliac-femoral artery to evaluate the percentage of the surface lesion area.

Iliac-femoral arteries were divided into 7 segments. The common iliac artery (from the branch of the aorta to the deep iliac artery) was designated as I-1. The orifice of the deep iliac artery to the orifice of the internal iliac artery was equally divided into three segments and was designated as I-2, I-3, and I-4 in order from the orifice of the deep iliac artery. The area from the orifice of the internal iliac artery to the branch of the deep femoral artery and the upper femoral artery was equally divided into three segments and designated as I-5, I-6, and I-7 in order from the orifice of the internal iliac artery.

Supplementary Table 1. Gender differences in the percentage of the surface lesion area of the thoracic aorta

	Ascending aorta	Aortic arch	Thoracic aorta 1	2	3	4	5	6	7	8	9
6 months old											
Female (n=2)	57±2	65±5	66±16	53±7	80±2	57±12	57±2	48±4	58±5	60±11	67±0
Male (n=5)	64±6	78±10	79±10	76±9	53±4	64±6	61±3	52±6	57±5	58±3	54±5
P-value											
12 months old											
Female (n=5)	81±2	77±2	79±1	76±2	70±4	74±3	71±5	64±6	64±5	63±6	56±5
Male (n=5)	65±7	80±1	81±2	81±2	73±1	68±4	76±4	64±5	63±7	74±4	74±5
P-value	0.094	0.306	0.472	0.149	0.583	0.236	0.448	1.000	0.857	0.163	0.049
20 months old											
Female (n=5)	82±3	87±3	79±2	76±3	81±3	83±1	80±3	73±2	79±2	75±2	75±3
Male (n=5)	83±3	85±1	81±2	77±4	78±2	78±3	82±2	80±2	77±1	81±2	80±3
P-value	0.762	0.564	0.518	0.793	0.475	0.141	0.688	0.045	0.398	0.105	0.213
30 months old											
Female (n=5)	90±1	91±3	87±2	85±3	85±4	87±1	83±2	79±4	81±3	81±5	79±4
Male (n=5)	88±2	90±3	86±2	86±4	91±2	87±2	81±3	82±2	81±4	83±5	76±2
P-value	0.473	0.876	0.706	0.933	0.246	0.988	0.550	0.552	0.998	0.727	0.501

Data are represented as the mean ± SEM. Statistical analyses were performed by Student's t-test or Welch's t-test.

Supplementary Table 2. Gender differences in the percentage of the surface lesion area of the abdominal aorta

	Abdominal aorta 1	2	3	4	5	6	7
6 months old							
Female (n=2)	40±8	35±1	37±7	22±12	11±4	8±1	28±10
Male (n=5)	42±2	38±2	36±9	19±7	16±6	5±3	11±7
P-value							
12 months old							
Female (n=5)	62±2	61±4	56±4	39±5	30±3	18±3	16±4
Male (n=5)	65±4	27±8	35±6	32±6	17±7	19±5	25±5
P-value	0.443	0.004	0.018	0.372	0.104	0.867	0.237
20 months old							
Female (n=5)	66±4	65±2	65±9	37±5	26±2	25±3	21±5
Male (n=5)	68±5	65±3	51±4	36±4	28±2	20±6	7±3
P-value	0.695	0.947	0.197	0.807	0.578	0.478	0.052
30 months old							
Female (n=5)	72±8	77±7	60±5	32±6	17±7	19±5	25±5
Male (n=5)	85±8	78±7	74±2	31±14	30±12	18±9	29±7
P-value	0.264	0.955	0.024	0.955	0.368	0.566	0.639

Data are represented as the mean ± SEM. Statistical analyses were performed by Student's t-test or Welch's t-test.

Supplementary Table 3. Gender differences in the percentage of the surface lesion area of the right carotid artery

	Proximal area	Middle area 1	Orifice of anterior thyroid artery	Middle area 2	Carotid sinus
6 months old					
Female (n=2)	10.8 ± 8.6	0.0 ± 0.0	9.7 ± 3.0	0.0 ± 0.0	4.0 ± 0.1
Male (n=5)	14.9 ± 5.8	0.0 ± 0.0	5.5 ± 1.8	0.0 ± 0.0	2.3 ± 1.0
P-value					
12 months old					
Female (n=5)	10.8 ± 1.4	0.0 ± 0.0	14.6 ± 0.6	0.0 ± 0.0	5.2 ± 2.3
Male (n=5)	17.6 ± 4.9	0.0 ± 0.0	11.4 ± 1.3	0.0 ± 0.0	2.9 ± 0.8
P-value	0.249		0.048		0.357
20 months old					
Female (n=5)	39.5 ± 4.9	13.0 ± 3.5	56.3 ± 5.7	20.4 ± 3.7	52.1 ± 7.6
Male (n=5)	44.9 ± 2.8	22.5 ± 1.5	71.9 ± 8.1	18.1 ± 4.6	48.6 ± 3.8
P-value	0.372	0.036	0.153	0.705	0.698
30 months old					
Female (n=5)	37.2 ± 2.1	24.6 ± 4.6	69.1 ± 8.2	28.1 ± 3.0	75.6 ± 7.3
Male (n=5)	44.3 ± 6.5	23.5 ± 4.9	71.0 ± 6.8	28.3 ± 4.0	76.6 ± 4.3
P-value	0.345	0.869	0.864	0.977	0.908

Data are represented as the mean ± SEM. Statistical analyses were performed by Student's t-test or Welch's t-test.

Supplementary Table 4. Gender differences in the percentage of the surface lesion area of the left carotid artery

	Proximal area	Middle area 1	Orifice of anterior thyroid artery	Middle area 2	Carotid sinus
6 months old					
Female (n=2)	7.9±7.9	0.0±0.0	18.1±1.7	6.2±2.1	24.2±3.9
Male (n=5)	4.1±2.4	1.2±1.2	15.3±6.0	0.3±0.3	26.5±10.8
P-value					
12 months old					
Female (n=5)	17.0±3.8	7.8±3.4	29.1±2.6	5.6±2.0	37.5±3.4
Male (n=5)	21.3±5.6	7.3±2.3	20.1±2.7	2.6±0.9	25.0±3.9
P-value	0.546	0.907	0.042	0.211	0.042
20 months old					
Female (n=5)	20.6±4.3	19.0±3.7	47.9±3.5	18.6±4.8	71.2±4.6
Male (n=5)	16.7±2.3	16.7±2.3	41.9±2.5	17.4±6.4	52.2±5.9
P-value	0.446	0.619	0.203	0.879	0.035
30 months old					
Female (n=5)	22.5±2.8	23.9±3.7	58.3±4.5	16.1±2.1	73.7±3.4
Male (n=5)	30.3±4.7	30.4±3.4	56.3±6.5	21.2±3.3	67.3±3.9
P-value	0.195	0.233	0.807	0.225	0.246

Data are represented as the mean ± SEM. Statistical analyses were performed by Student's t-test or Welch's t-test.

Supplementary Table 5. Gender differences in the percentage of the surface lesion area of the renal artery

	Right renal artery Proximal area	Middle area	Distal area	Left renal artery Proximal area	Middle area	Distal area
6 months old						
Female (n=2)	0.0 ± 0.0	0.0 ± 0.0	3.7 ± 3.7	0.0 ± 0.0	0.0 ± 0.0	0.0 ± 0.0
Male (n=5)	3.2 ± 2.4	0.0 ± 0.0	1.3 ± 1.3	1.1 ± 1.1	0.0 ± 0.0	0.0 ± 0.0
P-value						
12 months old						
Female (n=5)	9.5 ± 2.0	0.0 ± 0.0	6.2 ± 2.1	5.1 ± 1.6	0.0 ± 0.0	0.7 ± 0.7
Male (n=5)	8.9 ± 3.0	0.0 ± 0.0	8.9 ± 2.1	3.5 ± 1.2	0.0 ± 0.0	0.9 ± 0.9
P-value	0.865		0.377	0.441		0.838
20 months old						
Female (n=5)	9.9 ± 4.8	9.6 ± 3.2	15.5 ± 3.4	23.3 ± 1.3	0.3 ± 0.3	0.6 ± 0.0
Male (n=5)	15.8 ± 4.3	9.3 ± 2.9	10.3 ± 2.3	14.2 ± 1.3	2.7 ± 2.0	0.7 ± 0.0
P-value	0.383	0.936	0.240	0.001	0.257	0.384
30 months old						
Female (n=5)	29.0 ± 4.8	19.5 ± 3.7	32.6 ± 7.3	16.7 ± 3.9	12.7 ± 3.4	16.8 ± 4.4
Male (n=5)	36.9 ± 11.1	16.9 ± 2.1	33.5 ± 15.0	17.2 ± 3.1	5.2 ± 3.2	8.9 ± 4.1
P-value	0.531	0.559	0.959	0.924	0.148	0.224

Data are represented as the mean ± SEM. Statistical analyses were performed by Student's t-test or Welch's t-test.

Supplementary Table 6. Gender differences in the percentage of the surface lesion area of the pulmonary artery

	Pulmonary trunk	Pulmonary sinus	Right PA	Left PA
6 months old				
Female (n=2)	8.0±6.1	5.5±4.2	7.7±0.9	2.8±0.2
Male (n=5)	2.9±2.2	4.8±1.7	5.0±1.2	0.8±0.8
12 months old				
Female (n=5)	6.3±2.3	8.1±2.1	20.2±2.7	4.9±1.3
Male (n=5)	3.1±1.9	2.8±1.8	14.1±4.3	3.1±2.0
P-value	0.313	0.091	0.269	0.477
20 months old				
Female (n=5)	12.5±5.1	14.3±6.0	21.6±4.2	5.2±1.6
Male (n=5)	17.9±4.5	17.9±4.5	15.8±1.3	4.6±2.9
P-value	0.445	0.636	0.226	0.850
30 months old				
Female (n=5)	27.7±4.4	35.1±3.5	37.3±4.7	4.1±1.8
Male (n=5)	8.4±5.3	12.4±7.6	17.7±2.8	7.7±2.6
P-value	0.024	0.027	0.007	0.290

Data are represented as the mean±SEM. Statistical analyses were performed by Student's t-test or Welch's t-test.

Supplementary Table 7. Gender differences in the percentage of the surface lesion area of the iliac-femoral artery

	Right iliac-femoral artery			Left iliac-femoral artery		
	Common iliac artery	Branch of internal iliac artery	Femoral bifurcation	Common iliac artery	Branch of internal iliac artery	Femoral bifurcation
20 months old						
Female (n=5)	12.1 ± 2.7	4.6 ± 2.5	14.9 ± 4.5	5.8 ± 3.8	0.0 ± 0.0	9.2 ± 0.9
Male (n=5)	11.0 ± 2.6	7.7 ± 2.4	3.9 ± 3.9	0.0 ± 0.0	0.0 ± 0.0	10.0 ± 2.6
P-value	0.793	0.387	0.101	0.198		0.782
30 months old						
Female (n=5)	19.6 ± 5.2	18.3 ± 1.0	9.7 ± 4.9	23.8 ± 2.4	14.1 ± 4.2	18.2 ± 5.0
Male (n=5)	14.6 ± 4.8	10.0 ± 6.2	5.4 ± 3.4	10.5 ± 4.3	18.6 ± 3.7	12.0 ± 4.2
P-value	0.498	0.252	0.488	0.028	0.437	0.367

Data are represented as the mean ± SEM. Statistical analyses were performed by Student's t-test or Welch's t-test.

Supplementary Table 8. Serum lipid levels of WHHLMI rabbits

	Age (months) 3	6	12	18	24	30
Total cholesterol (mg/dl)						
Female	883 ± 22 (n=17)	1131 ± 29 (n=17)	968 ± 49 (n=13)	892 ± 37 (n=9)	835 ± 51 (n=5)	889 ± 24 (n=3)
Male	895 ± 19 (n=20)	1122 ± 30 (n=20)	821 ± 44 (n=11)	759 ± 64 (n=10)	666 ± 20 (n=5)	673 ± 39 (n=3)
P-value	0.684	0.842	0.039	0.100	0.015	0.009
Triglyceride (mg/dl)						
Female	321 ± 20 (n=17)	231 ± 17 (n=17)	262 ± 21 (n=13)	231 ± 19 (n=9)	232 ± 30 (n=5)	228 ± 16 (n=3)
Male	281 ± 16 (n=20)	208 ± 15 (n=20)	264 ± 27 (n=11)	230 ± 25 (n=10)	194 ± 21 (n=5)	167 ± 22 (n=3)
P-value	0.130	0.326	0.954	0.985	0.331	0.089

Data are represented as the mean ± SEM. Statistical analyses were performed by Student's t-test.

Supplementary Table 9. *P*-values by Tukey test for the percentage of the surface lesion area in aortas among groups

	AsA	AA	T-1	T-2	T-3	T-4	T-5	T-6	T-7	T-8	T-9	A-1	A-2	A-3	A-4	A-5	A-6	A-7
6 months old vs.																		
12 months old	0.106	0.820	0.773	0.358	0.095	0.114	0.002	0.020	0.491	0.241	0.524	0.003	0.751	0.607	0.181	0.529	0.118	0.888
20 months old	<0.001	0.653	0.779	0.569	0.002	0.002	<0.001	<0.001	<0.001	0.005	0.003	<0.001	0.002	0.022	0.141	0.265	0.028	0.995
30 months old	<0.001	0.006	0.098	0.025	<0.001	<0.001	<0.001	<0.001	<0.001	<0.001	0.002	<0.001	<0.001	<0.001	0.417	0.535	0.137	0.321
12 months old vs.																		
20 months old	0.110	0.251	1.000	0.978	0.278	0.049	0.121	0.037	0.006	0.228	0.047	0.894	0.014	0.204	0.999	0.947	0.719	0.717
30 months old	0.003	0.028	0.401	0.465	0.004	<0.001	0.063	0.003	0.008	0.046	0.034	0.032	<0.001	0.011	0.939	1.000	0.081	0.679
20 months old vs.																		
30 months old	0.416	0.717	0.395	0.258	0.239	0.285	0.979	0.796	0.875	0.849	0.999	0.146	0.197	0.550	0.887	0.944	0.853	0.151

AsA, ascending aorta; AA, aortic arch; T-1-T-9, thoracic segments 1-9 from the proximal to the distal region; A-1 to A-7, abdominal segments 1-7 from the proximal to the distal region.

Supplementary Table 10. *P*-values by Tukey test for the percentage of the surface lesion area in carotid arteries among groups

	Right-1	Right-2	Right-3	Right-4	Right-5	Left-1	Left-2	Left-3	Left-4	Left-5
6 months old vs.										
12 months old	1.000	1.000	0.726	1.000	0.993	0.020	0.171	0.280	0.934	0.849
20 months old	<0.001	<0.001	<0.001	<0.001	<0.001	0.004	<0.001	<0.001	<0.001	<0.001
30 months old	<0.001	<0.001	<0.001	<0.001	<0.001	<0.001	<0.001	<0.001	<0.001	<0.001
12 months old vs.										
20 months old	<0.001	<0.001	<0.001	<0.001	<0.001	0.891	0.006	<0.001	0.001	<0.001
30 months old	<0.001	<0.001	<0.001	<0.001	<0.001	0.308	<0.001	<0.001	<0.001	<0.001
20 months old vs.										
30 months old	0.988	0.159	0.698	0.012	<0.001	0.720	0.014	0.029	0.998	0.469

Right-1, proximal area of right carotid artery; Right-2, area between Right-1 and Right-3; Right-3, area around orifice of anterior thyroid artery; Right-4, area between Right-3 and Right-5; Right-5, sinus of right carotid artery; Left-1, proximal area of left carotid artery; Left-2, area between Left-1 and Left-3; Left-3, area around orifice of anterior thyroid artery; Left-4, area between Left-3 and Left-5; Left-5, sinus of left carotid artery.

Supplementary Table 11. Differences in the percentage of surface lesion area between right and left carotid arteries

	Proximal area	Middle area 1	Orifice of anterior thyroid artery	Middle area 2	Carotid sinus	Whole artery
6 months old (n=7)						
Left CA	5.2 ± 2,5	0.9 ± 0.9	16.1 ± 4.2	1.9 ± 1.2	25.9 ± 7.5	10.0 ± 2.5
Right CA	13.7 ± 4.5	0.0 ± 0.0	6.7 ± 1.6	0.0 ± 0.0	2.8 ± 0.8	4.6 ± 0.7
P-value	0.123	0.366	0.071	0.167	0.022	0.078
12 months old (n=10)						
Left CA	19.2 ± 3.3	7.6 ± 1.9	24.6 ± 2.3	4.1 ± 1.2	31.2 ± 3.2	17.3 ± 1.3
Right CA	14.2 ± 2.7	0.0 ± 0.0	13.0 ± 0.9	0.0 ± 0.0	4.0 ± 1.2	6.3 ± 0.6
P-values	0.254	0.004	<0.001	<0.001	<0.001	<0.001
20 months old (n=10)						
Left CA	22.1 ± 3.0	17.8 ± 2.1	44.9 ± 2.3	18.0 ± 3.8	61.7 ± 4.8	32.9 ± 1.8
Right CA	42.2 ± 2.8	17.7 ± 2.4	64.1 ± 5.4	19.3 ± 2.8	50.4 ± 4.1	38.7 ± 1.8
P-value	<0.001	0.978	0.006	0.787	0.087	0.036
30 months (n=10)						
Left CA	26.4 ± 2.9	27.2 ± 2.6	57.3 ± 3.7	18.6 ± 2.0	70.5 ± 2.7	40.0 ± 1.9
Right CA	40.8 ± 3.4	24.0 ± 3.2	70.1 ± 5.0	28.2 ± 2.5	76.1 ± 4.0	47.8 ± 1.9
P-value	0.005	0.059	0.057	0.007	0.261	0.010

Data are represented as the mean ± SEM. Statistical analyses were performed by Student's t-test or Welch's t-test.
CA, carotid artery

Supplementary Table 12. *P*-values by Tukey test for percentage of the surface lesion area in pulmonary arteries among groups

	Pulmonary trunk	Pulmonary sinus	Right pulmonary artery	Left pulmonary artery
6 months old vs.				
12 months old	1.000	1.000	0.071	0.597
20 months old	0.731	0.207	0.032	0.352
30 months old	0.004	0.010	<0.001	0.160
12 months old vs.				
20 months old	0.716	0.170	0.981	0.966
30 months old	0.024	0.005	0.068	0.759
20 months old vs.				
30 months old	0.220	0.434	0.148	0.954

Supplementary Table 13. Differences in the percentage of the surface lesion area between right and left pulmonary arteries and renal arteries

	Pulmonary artery	Renal artery Proximal area	Middle area	Distal area	Whole artery
6 months old (n=7)					
Left	1.4 ± 0.7	0.8 ± 0.8	0.0 ± 0.0	0.0 ± 0.0	0.3 ± 0.3
Right	5.8 ± 1.0	2.3 ± 1.7	0.0 ± 0.0	2.0 ± 1.3	1.4 ± 0.6
P-value	0.003	0.463		0.174	0.105
12 months old (n=10)					
Left	4.0 ± 1.1	4.3 ± 1.0	0.0 ± 0.0	0.8 ± 0.5	1.7 ± 0.3
Right	17.1 ± 2.6	9.2 ± 1.7	0.0 ± 0.0	7.6 ± 1.5	5.6 ± 0.6
P-values	<0.001	0.022		0.001	<0.001
20 months old (n=10)					
Left	4.9 ± 1.6	18.7 ± 1.7	1.5 ± 1.0	0.6 ± 0.0	7.0 ± 0.5
Right	18.7 ± 2.3	12.9 ± 3.2	9.4 ± 2.0	12.9 ± 2.1	11.7 ± 1.7
P-value	<0.001	0.124	0.003	<0.001	0.025
30 months old (n=10)					
Left	5.9 ± 1.6	16.9 ± 2.3	8.9 ± 2.5	12.8 ± 3.1	12.9 ± 1.6
Right	27.5 ± 4.2	33.0 ± 5.9	18.2 ± 2.0	33.1 ± 7.9	28.1 ± 4.0
P-value	<0.001	0.026	0.011	0.035	0.004

Data are represented as the mean ± SEM. Statistical analyses were performed by Student's t-test or Welch's t-test.

Supplementary Table 14. *P*-values by Tukey test for the percentage of the surface lesion area in renal arteries among groups

	Right-1 Proximal area	Right-2 Middle area	Right-3 Distal area	Left-1 Proximal area	Left-2 Middle area	Left-3 Distal area
6 months old vs.						
12 months old	0.618	1.000	0.841	0.530	1.000	0.989
20 months old	0.259	0.002	0.385	<0.001	0.904	0.994
30 months old	<0.001	<0.001	<0.001	<0.001	0.002	<0.001
12 months old vs.						
20 months old	0.889	<0.001	0.821	<0.001	0.876	1.000
30 months old	<0.001	<0.001	0.001	<0.001	<0.001	<0.001
20 months old vs.						
30 months old	0.002	0.001	0.012	0.863	0.005	<0.001

Supplementary Table 15. *P*-values by Tukey test for the percentage of the surface lesion area in iliac-femoral arteries

	Right-1 Common iliac artery	Right-4 Around orifice of internal iliac artery	Right-7 Branching site of deep femoral artery	Left-1 Common Iliac artery	Left-4 Around orifice of internal iliac artery	Left-7 Branching site of deep femoral artery
6 months old vs.						
12 months old	1.000	1.000	1.000	1.000	1.000	1.000
20 months old	0.005	0.188	0.063	0.781	1.000	0.010
30 months old	<0.001	<0.001	0.177	<0.001	<0.001	<0.001
12 months old vs.						
20 months old	0.002	0.127	0.034	0.727	1.000	0.004
30 months old	<0.001	<0.001	0.117	<0.001	<0.001	<0.001
20 months old vs.						
30 months old	0.222	0.027	0.942	<0.001	<0.001	0.160

Supplementary Table 16. Differences in the percentage of the surface lesion area between right and left iliac-femoral arteries

	Common iliac artery	Branch of internal iliac artery	Femoral bifurcation	Whole artery
20 months old (n=10)				
Left	2.9 ± 2.0	0.0 ± 0.0	9.6 ± 1.3	1.8 ± 0.3
Right	11.5 ± 1.8	6.1 ± 1.7	9.4 ± 3.4	3.9 ± 0.5
P-value	*0.005*	*0.006*	*0.966*	*0.001*
30 months (n=10)				
Left	17.1 ± 3.2	16.4 ± 2.7	15.1 ± 3.2	6.9 ± 0.7
Right	17.1 ± 3.4	14.2 ± 3.3	7.5 ± 2.9	5.6 ± 0.7
P-value	*1.000*	*0.618*	*0.100*	*0.172*

Data are represented as the mean ± SEM. Statistical analyses were performed by Student's t-test or Welch's t-test.